Applied Catalysis, 57 (1990) 223–240
Elsevier Science Publishers B.V., Amsterdam — Printed in The Netherlands

Effect of Fluorine on Hydrogenation of Cyclohexene on Sulfided Ni (or Co)–Mo/Al_2O_3 Catalysts

J. RAMIREZ and R. CUEVAS

Departamento de Ingeniería Química, Facultad de Química, UNAM, Ciudad Universitaria, México, D.F. 04510 (México)

and

A. LÓPEZ AGUDO*, S. MENDIOROZ and J.L.G. FIERRO

Instituto de Catálisis y Petroleoquímica, CSIC, Serrano, 119, 28006 Madrid (Spain)

(Received 26 June 1989, revised manuscript received 12 September 1989)

ABSTRACT

The effect of fluorine incorporation on alumina support on the surface structure of unpromoted molybdenum, promoted cobalt–molybdenum and nickel–molybdenum catalysts, and their activity for hydrogenation of cyclohexene has been studied. The incorporation of 0.2 and 0.8 wt.-% fluorine on the alumina was carried out by impregnation with NH_4F solutions. The catalysts in the oxidic state were characterized by X-ray diffraction and ammonia adsorption and in the sulfide state by X-ray photoelectron spectroscopy (XPS) and infra-red spectroscopy (IR) of adsorbed NO. The absence of significant changes in the binding energy values of Mo3d and Ni2p (or Co2p) levels in the XPS spectra of the fluorine-containing catalysts as compared to the fluorine-free counterpart does not support the existence of an electronic effect of fluorine. The quantitative XPS results showed, however, that fluorine clearly increases the dispersion of molybdenum and promoter, this being linearly correlated to surface fluorine content. The IR results of adsorbed NO also indicate that fluorine incorporation leads generally to minor sizes of MoS_2 slabs, and more exposed promoter atoms, except for the cobalt in the Co–Mo/F(0.2)A catalyst. It is suggested that the increase in the dispersion of the supported active phase is a secondary effect of fluorine incorporation, which may result from the observed textural changes of the alumina and its small partial solubilization provoked by NH_4F solution. It was found that the incorporation of fluorine enhances appreciably, moderately and considerably the hydrogenation activity of molybdenum, cobalt–molybdenum an nickel–molybdenum catalysts, respectively. Such increase in hydrogenation activity is not directly correlated to the exposed atoms probed by NO adsorption, and is only loosely related to molybdenum dispersion for the molybdenum and cobalt–molybdenum catalysts. The lack of similar reliable correlations for the nickel–molybdenum catalysts suggests that other structural parameters such as extent of reduction–sulfidation and certain configurations of molybdenum ions and sulfur vacancies may govern hydrogenation activity.

0166-9834/90/$03.50

INTRODUCTION

During the last five years extensive research has been carried out on the influence of fluorine incorporation in Co/Al_2O_3 and $Ni–Mo/Al_2O_3$ catalysts on their surface and catalytic properties [1–12]. The interest in these studies has essentially emerged from the increasing industrial requirement for more effective catalysts for refining heavy crude oil fractions with high nitrogen contents. It is well know that fluorination of alumina increases its surface acidity [2,6,13,14] and therefore enhances acid-catalysed reactions. On the other hand, surface acidity seems to be a key parameter for C–N bond cleavage reactions [15–17]. It is also known that removal of nitrogen from the heterocyclic molecules involves ring hydrogenation prior to C–N bond hydrogenolysis. However, most of the reported studies on fluorine-containing hydrotreating catalysts have centered on the effect of fluorine on both cracking and hydrocracking [1,5–8] as well as on hydrodesulphurization (HDS) [1,4,9–12] activities. Relatively little attention has been paid to the effect of fluorine on hydrodenitrogenation (HDN) [1] and hydrogenation [8,9] functionalities of such catalysts. Boorman et al. [8] reported that fluorine addition to $Co–Mo/Al_2O_3$ catalysts increased cyclohexene isomerization and inhibited cyclohexene hydrogenation; only on fluorine-free $Co–Mo/Al_2O_3$ catalysts was a significant amount of cyclohexane (ca. 2.4% of yield) obtained. However, Jiratova and Kraus [9] reported that the addition of 3 wt.-% fluorine increased substantially both isomerisation and hydrogenation of cyclohexene, as well as HDS of thiophene. Some of these differences could be attributed to differences in the method of preparation and/or in the percentage of fluorine incorporated. Another possible explanation for such differences would reside in the nature of the promoter. Therefore, it was of interest to compare Co–Mo and Ni–Mo catalysts prepared following similar preparation method.

In the present work we studied the catalytic behaviour, for cyclohexene transformation, of $Co–Mo/Al_2O_3$ and $Ni–Mo/Al_2O_3$ catalysts containing various amounts of fluorine. For comparison, fluorine-containing Mo/Al_2O_3 and Ni/Al_2O_3 catalysts were also examined. Characterization of the catalysts was carried out using several techniques including, X-ray diffraction, infra-red spectroscopy of adsorbed NO, X-ray photoelectron spectroscopy and acidity measurements.

EXPERIMENTAL

Catalyst preparation

A γ-Al_2O_3 (Girdler T-126, BET surface area 190 $m^2\ g^{-1}$; pore volume, 0.39 $cm^3\ g^{-1}$; particle size, 100 mesh) was impregnated firstly with aqueous solutions of NH_4F (Merck, reagent grade) of the appropriate concentration to

yield samples containing 0.2 and 0.8 wt.-% fluorine. As the pore filling method was used in all preparations, a volume of solution equal to the pore volume of Al_2O_3 plus a 10% excess was employed. After drying at 393 K for 12 hours, the impregnates were calcined at 723 K for 4 hours. These alumina-modified samples, denoted by F(x)A, were then used to prepare a series of Mo-, Ni–Mo- and Co–Mo-containing catalysts by the dry impregnation method: $(NH_4)_6Mo_7O_{24}\cdot 4H_2O$, $Ni(NO_3)_2\cdot 6H_2O$ and $Co(NO_3)_2\cdot 6H_2O$ (all Merck, reagent grade) were used as precursors of the active components. The promoted catalysts were prepared by depositing first molybdenum and then cobalt or nickel. After molybdenum impregnation the precursor solid was dried at 393 K for 18 hours and then calcined at 623 K for 4 hours. The promoter-impregnated samples were also dried at 393 K for 18 hours and calcined at 723 K for 4 hours. Another fluorine-free series of catalysts were prepared following the same procedure as above. The loadings of catalysts expressed as percentages of metal oxides were as follows: 12.0 wt.-% MoO_3, 2.8 wt.-% CoO and 6.5 wt.-% NiO. The catalysts will be referenced to hereafter as: Mo/F(x)A, Ni–Mo/F(x)A and Co–Mo/F(x)A, where $x=0.0$, 0.2 or 0.8, denoting fluorine weight percentage.

Catalytic activity

Catalytic activity measurements for cyclohexene hydrogenation were carried out in a Parr autoclave operating in a batch mode at 6.28 MPa hydrogen pressure and various temperatures in the range 573–673 K. Prior to each catalytic run, the samples were presulfided in a separate fixed-bed microreactor with a 10% (v/v) H_2S/H_2 mixture at 673 K for 4 hours. Unreacted cyclohexene and reaction products were analysed by gas chromatography using a 10% Carbowax 20M of 100/120 Chromosorb W HP column (4 m×1/8″ O.D.). Reaction rates for cyclohexene hydrogenation (r_{HYD}) and isomerization (r_{ISO}) reactions were calculated from cyclohexene conversions to cyclohexane and methylcyclopentene isomers, respectively, measured after a 4-h run.

Catalyst characterization

The X-ray diffraction patterns were recorded using a Philips PW 1730/10 diffractometer using Ni-filtered CuKα radiation, under constant instrumental parameters.

The determination of acidity of the oxidic precursors was based on measurements of ammonia adsorption. The ammonia adsorption–desorption profiles were automatically monitored by microgravimetry on a Perkin Elmer thermoanalyser interfaced to a data system. The samples were heated at a rate of 10 K min^{-1} until 723 K in a nitrogen stream and allowed to cool down to room temperature. Then a 1:1 (v/v) NH_3–N_2 mixture was introduced and the

extent of ammonia adsorption measured when equilibrium was attained. Ammonia was subsequently desorbed by temperature programming (10 K min^{-1}) up to a final temperature of 723 K in a nitrogen flow. The number of acid sites, expressed as μmole NH_3 per gram, was calculated from the extent of ammonia adsorption at room temperature.

Infrared experiments were carried out in a special cell, assembled with greaseless stopcocks and KBr windows, which permitted either static or dynamic treatments. The sulfide samples were pressed into very thin waters (thickness: 10.0–11.6 mg cm^{-2}). These samples were purged with helium at 673 K for 0.5 hour and then resulfided in situ with a 10% (v/v) H_2S–H_2 mixture for 1 hour at the same temperature. After purging the cell with helium, the samples were heated at 773 K and outgassed for 1 hour, then cooled to room temperature. They were subsequently contacted with 4.0 kPa NO for 0.5 hour. All spectra were recorded on a Nicolet ZDX FTIR spectrophotometer at a resolution of 2 cm^{-1}.

X-ray photoelectron spectra (XPS) were obtained by using a Leybold Heraeus LHS 10 spectrometer with a hemispherical electron analyser and a magnesium X-ray excitating source (MgKα = 1253.6 eV). The powdered samples were sulfided separately in a 10% (v/v) H_2S–H_2 mixture at 673 K for 4 hour, and then collected under iso-octane and pressed into small holders under the meniscus of iso-octane to prevent oxidation by air. These holders were fixed to a long rod placed in an introduction chamber. The samples were outgassed down to 10^{-3} Pa before they were moved into the analysis chamber. The pressure in this turbopumped main vacuum chamber was maintained at ca. $5 \cdot 10^{-7}$ Pa during data acquisition. Each spectral region was signal averaged for a number of scans to obtain good signal-to-noise ratios. Although surface charging was observed in all samples, accurate binding energies (BE) could be determined by charge referencing with the adventitious Al 2p line at 74.7 eV.

RESULTS

X-ray diffraction (XRD) and specific surface areas

Examination of XRD spectra of the oxidic precursors of the catalyst studied revealed only diffraction lines characteristic of γ-Al_2O_3. Other crystalline structures at the XRD scale (i.e. ca. 4 nm crystal size), such as AlF_3, MoO_3, Co_3O_4, NiO or any other defined compounds from binary combinations, were not detected.

Surface area of the unmodified alumina decreased slightly from 190 $m^2 g^{-1}$ to 177 and 174 $m^2 g^{-1}$ for the fluorine-modified samples F(0.2)A and F(0.8)A, respectively. Although these variations are within the experimental error of the technique, the tendency can be considered significant, as it follows the same trend usually observed in other works in which a larger range of fluorine-

containing samples were studied [11,12,14,18,19]. In agreement with the literature findings for fluorinated alumina [14], the loss of surface area can be primarily associated with a partial dissolution of the Al_2O_3 at the thin walls between micropores by NH_4F. This was supported by comparing the low relative pressure regions of the nitrogen adsorption–desorption isotherms of the F(0.0)A and F(0.8)A samples, and their pore-radius distribution. Both average and mode pore radius were ca. 0.5 and 0.7 nm, respectively, larger for the F(0.8)A sample.

It should be mentioned that the surface areas of Mo/F(x)A and Ni(or Co)–Mo/F(x)A catalysts were essentially the same as those of the F(x)A counterparts.

Acidity

The dependence of surface acidity, as estimated by ammonia adsorption, and fluorine content for the F(x)A, Mo/F(x)A and M–Mo/F(x)A (M=Co or Ni) catalyst series is shown in Fig. 1. As expected, fluorine incorporation produced a marked enhancement of alumina acidity, with a maximum generally for the 0.2 wt.-% preparation. In agreement with results of other studies [2,6,20–23], a much more pronounced acidity increase is observed after molybdenum incorporation on the fluorine-free and fluorinated aluminas. Subsequent incorporation of promoter (Ni or Co) brings about additional acidity changes. In the case of Ni, the acidity of the Ni–Mo/F(x)A preparations was slightly higher than that of the Mo/F(x)A counterparts. On the contrary, cobalt incorporation in the Mo/F(x)A preparations resulted in a marked acidity decrease, although it was always maintained above that of the F(x)A preparations. This finding agrees with some literature data in that addition of cobalt to Mo/Al_2O_3 base catalysts destroys Brönsted acid sites associated to the MoO_3 phase [6,20,22]. In general, the changes in acidity caused by addition of cobalt or

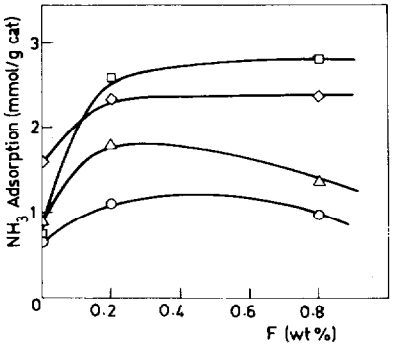

Fig. 1. Dependence of ammonia adsorption capacity at room temperature on fluorine content in catalysts: (○)F(x)A; (◇)Mo/F(x)A; (□)Ni–Mo/F(x)A; (△)Co–Mo/F(x)A.

nickel to Mo/F(x)A samples are likely to be associated with the arrangement of molybdenum and cobalt or nickel species on alumina and the interaction between Co (or Ni) and Mo species, as previously suggested [20,22].

IR of adsorbed NO

IR spectroscopy of the NO molecule adsorbed on sulfided hydrotreating catalysts has been established as a powerful technique to give valuable information on the structure of promoter and molybdenum ions (see, e.g., ref. 24 and references therein). The IR spectra of NO adsorbed on sulfided Mo/F(x)A and M–Mo/F(x)A (M=Co or Ni) catalyst series are given in Fig. 2.

Adsorption of NO on sulfided Mo/F(x)A catalyst series gave rise to the

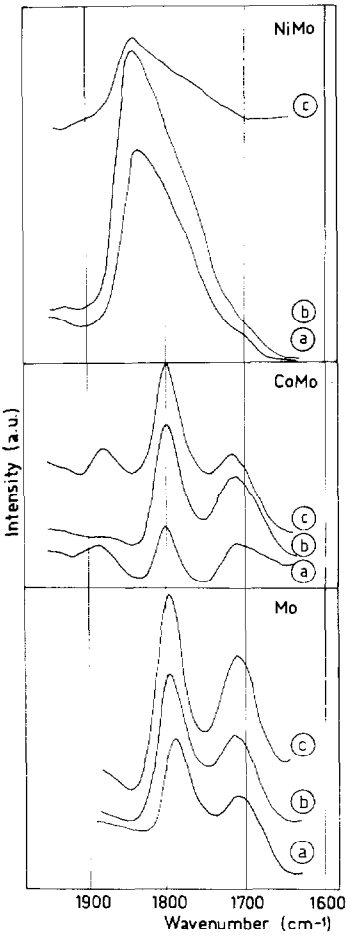

Fig. 2. IR of adsorbed NO on sulfided catalysts: (a) F(0.0)A; (b) F(0.2)A; and (c) F(0.8)A.

characteristic doublet at 1710 and 1800 cm^{-1} arising from NO pairs, either in a dimeric or dynitrosyl configuration. It is clear from Fig. 2 that fluorine content did not influence band position, although significant intensity changes were observed. For the promoted M–Mo/F(x)A (M=Co or Ni) catalysts. The bands of NO adsorbed on Co^{2+} at about 1800 and 1880 cm^{-1}, on Ni^{2+} at ca. 1846 cm^{-1}, and on $Mo^{\delta+}$ sites ($\delta<5$), if any, at 1710 and 1800 cm^{-1}, are similar to those reported in the literature [24,25]. In the case of Ni–Mo/F(x)A catalysts, a very intense and broad band centered at ca. 1846 cm^{-1} and a small shoulder at ca. 1700 cm^{-1} are observed. Since the band at 1700 cm^{-1} is due exclusively to $Mo^{\delta+}$ sites, it indicates that only a small fraction of these sites are exposed. However, the broadening and asymmetry on the lower wavenumber side of the and at ca. 1846 cm^{-1} indicates the presence of adsorbed NO, mostly as monomeric NO adsorbed species, and probably including a certain proportion of highly distorted trans-dimer $(NO)_2$ species.

To get some insight on the changes of NO adsorption induced by the fluorine incorporation to the catalysts, the absorbance of characteristic NO bands is plotted as a function of the fluorine content (Fig. 3). As can be seen, the absorbance of NO adsorbed on sulfide $Mo^{\delta+}$ sites for both the Mo/F(x)A and Co–Mo/F(x)A series (Fig. 3a), on sulfide Ni^{2+} sites for the Ni–Mo/F(x)A series (Fig. 3b), and on sulfide Co^{2+} sites for the Co–Mo/F(x)A series (Fig.

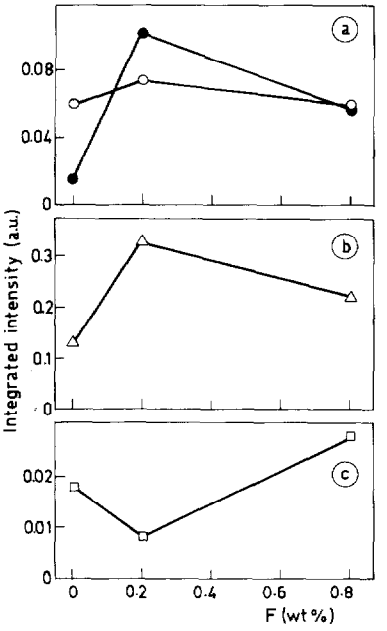

Fig. 3. Absorbance of the bands of NO adsorbed on: (a) Mo where (○) = Mo/F(x)A and (●) = Co–Mo/F(x)A; (b) Ni; and (c) Co, for sulfided catalysts as a function of fluorine content.

3c), depends markedly on the fluorine content of catalysts. In general, the absorbance of NO on sulfide $Mo^{\delta+}$, Ni^{2+} and Co^{2+} sites increases for the F(0.8)A preparations with respect to the fluorine-free counterparts (the only exception is the Mo/F(x)A series whose absorbances did not change significantly). However, the most important changes occurred on Mo/(0.2)A, CoMo F(0.2)A and Ni–Mo/F(0.2)A specimens. For instance, absorbance increased for NO adsorbed on $Mo^{\delta+}$ sites, in both Mo/F(0.2)A and Co–Mo/F(0.2)A catalyst, and on Ni^{2+} sites, in Ni–Mo/F(0.2)A catalyst, while it was much lower on Co^{2+} sites in Co–Mo/F(0.2)A preparation. In principle, this latter result seems somewhat striking, but a careful inspection of spectrum line shape reveals a much higher exposition of $Mo^{\delta+}$ sites (doublet at 1800–1710 cm^{-1}) than of Co^{2+} sites (doublet at 1880–1800 cm^{-1}). This strong inhibition of NO adsorption on sulfide Co^{2+} sites in Co–Mo/F(0.2)A preparation suggests that most of the Co^{2+} incorporated during preparation is lost by formation of tetrahedrally coordinated $CoAl_2O_4$-like species at the alumina interface during the calcination step, which are then difficult to sulfide.

X-ray photoelectron spectra

The Mo 3d and S 2s region of the photoelectron spectrum has been recorded for all catalysts. The Mo 3d doublet is rather well resolved (Fig. 4) and the BE values for the Mo $3d_{5/2}$ and Mo $3d_{3/2}$ levels were 229.1 and 232.2 eV, respectively, which fit well with literature data for MoS_2 species [26,27]. Although a small S 2s peak is observed on the lower BE side of the Mo $3d_{5/2}$ peak, no further attention will be paid to this line. Table 1 and Fig. 4 show that BE values remain essentially unchanged, within the accuracy of the spectrometer, whatever the fluorine content. When the $Mo3d_{5/2}/Mo3d_{3/2}$ intensity ratio is calculated for all preparations, a minimum is found for the F(0.2) catalysts while it increases slightly for F(0.8) preparations with respect to the F(0.0) counterparts. This would indicate that fluorination up to ca. F(0.2) inhibits the extent of sulfidation and/or reduction (higher BE values) of Mo^{6+} species.

Some differences are also observed in the BE of Co $2p_{3/2}$ and Ni $2p_{3/2}$ levels in the promoted catalysts. An examination of the data in Table 1 reveals that the BE depends to some extent on the fluorine content of the catalysts. For the Co–Mo/F(x)A series the highest BE corresponds to the preparation F(0.2), while it decreases for F(0.0), and decreases much more for F(0.8) preparations. For the Ni–Mo/F(x)A series, these differences, if any, are much smaller. In addition, no significant changes were found in the BE of O1s, S2p and F1s levels.

To get an idea of the relative abundance of the surface Mo and promoter (Co or Ni) ions as well as of the possible changes introduced by fluorine incorporation, the XPS intensities of the Mo 3d relative to the Al 2p peak have been calculated and plotted with that of the F 1s relative to Al 2p peak (Fig.

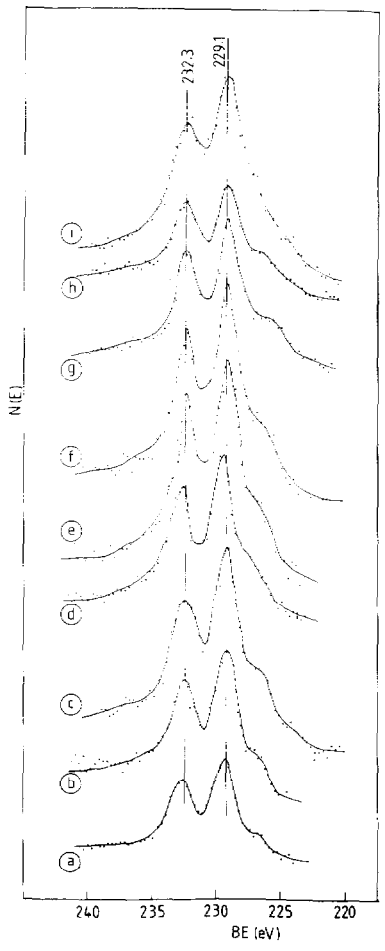

Fig. 4. XP spectra of the Mo 3d and S 2s levels for the sulfided catalysts: (a) Mo/F(0.0)A; (b) Mo/F(0.2)A; (c) Mo/F(0.8)A; (d) Co-Mo/F(0.0)A; (e) Co-Mo/F(0.2)A; (f) Co-Mo/F(0.8)A; (g) Ni-Mo/F(0.0)A; (h) Ni-Mo/F(0.2)A; and (i) Ni-Mo/F(0.8)A.

5a). A similar plot of the XPS intensities of the M 2p (M=Ni or Co) relative to Al 2p peak versus that of the F 1s relative to Al 2p peak is given in Fig. 5b. For the promoter-free preparations, Mo/F(x)A series, the ratio of Mo-to-Al intensities is very high, increasing slightly with F-to-Al ratio. The Mo-to-Al ratio for the Mo/F(0)A preparation is a somewhat higher (31%) than that predicted by the model of Kerkhoff and Moulijn [28]. This indicates that molybdenum oxide is not homogeneously distributed over the alumina surface: the external surface of the catalyst grains became Mo-enriched during preparation. It is suggested that a small fraction of the molybdate solution filling the pores is carried away from the pores during the drying step where molybdate

TABLE 1

Binding energies (eV) of several atomic levels for sulfided catalysts
All binding energies were referenced to the Al2p peak at 74.7 eV

Sample	O1s	$Mo3d_{5/2}$	S2p	$Co2p_{3/2}$	$Ni2p_{3/2}$	F1s
Mo/F(0)A	531.4	228.9	162.0	–	–	–
Mo/F(0.2)A	531.7	229.0	162.2	–	–	685.7
Mo/F(0.8)A	531.4	228.9	162.0	–	–	685.2
Co/Mo/F(0)A	531.6	229.4	162.6	779.6	–	–
CoMo/F(0.2)A	531.6	229.1	162.7	780.7	–	685.3
CoMo/F(0.8)A	531.2	229.0	162.3	778.7	–	685.1
NiMo/F(0)A	531.3	229.1	162.3	–	854.1	–
NiMo/F(0.2)A	531.6	229.2	161.9	–	853.7	685.6
NiMo/F(0.8)A	531.8	229.0	162.0	–	853.8	685.6

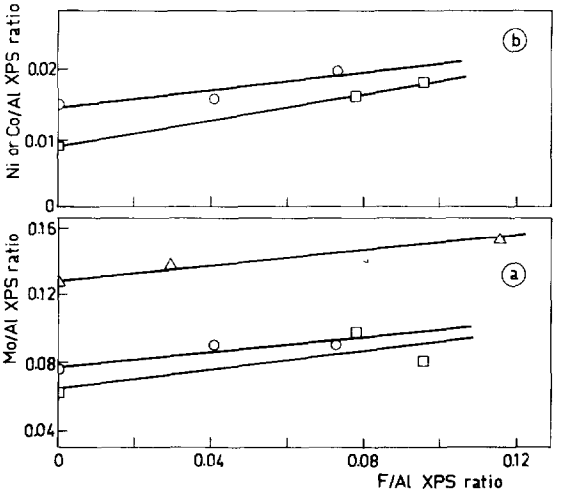

Fig. 5. Correlation between (a) Mo-to-Al, (b) Ni (or Co)-to-Al and F-to-Al XPS ratios. Catalyst series: (△) Mo/F(x)A; (○) NiMo/F(x)A; (□) CoMo/F(x)A.

precipitates, thus producing Mo surface enrichment. A similar effect has been found recently for other molybdenum-based catalysts prepared from the same molybdate precursors [29,30]. For promoted catalysts, Mo-to-Al ratios also increase with F-to-Al ratios, but the relative values were much lower, 40% and 46% for the NiMo/F(x)A and CoMo/F(x)A preparations, respectively (Fig. 5a). The same tendency is observed for the M-to-Al (M=Ni or Co) intensity ratios when they plotted against F-to-Al (Fig. 5b), although in this case the M-to-Al ratios are lower by a factor of ca. 6. As the F-to-Al intensity ratio is a

measure of the fluorine concentration at the alumina surface, both the molybdenum and promoter exposures increase with fluorine concentration.

Catalytic activity

Cyclohexene conversion at 573 K on the Ni–Mo/F(x) catalyst series is given in Fig. 6 as function of reaction time. Similar trends were generally observed on the other catalyst series. The reaction products over Ni(Co)–Mo/F(x)A catalysts were essentially cyclohexane; traces of methylcyclopentene isomers were also found in some cases, generally on F(0.8) samples and at reaction temperatures higher than 613 K. The variations of the reaction rate for hydrogenation of cyclohexene to cyclohexane (r_{HYD}) determined at various temperatures as a function of F(x) for Ni–MO/F(x)A and Co–Mo/F(x)A catalysts are presented in Fig. 7a and 7b, respectively. Hydrogenation activity increased for F(0.2) preparations, but it leveled off at higher fluorine contents. It should be noted that the increase in activity caused by fluorination was relatively larger for the Ni-promoted than for the Co-promoted catalysts. In fact, it can be seen from Figs. 7a and 7b that the activity of the Ni–Mo/(x)A catalysts increased by a factor of ca. 4 with respect to its fluorine-free counterpart, while the activity of the Co–Mo/F(x)A catalysts increased by a factor of 1.5 relative to its fluorine-free homologue.

For the unpromoted Mo/F(0.0)A catalyst, the principal reaction observed was also hydrogenation, but isomerization was always detected although to a neglibible extent. Similarly to the fluorine-containing promoted Mo catalysts, the other two Mo/F(x)A (x=0.2 and 0.8) catalysts showed slightly increased hydrogenation activity (Fig. 7c). However, the most important difference between the Mo/F(0.0)A and Mo/F(x)A (x=0.2, 0.8) catalysts is that the isomerization reaction increased greatly for fluorinated samples. This effect of

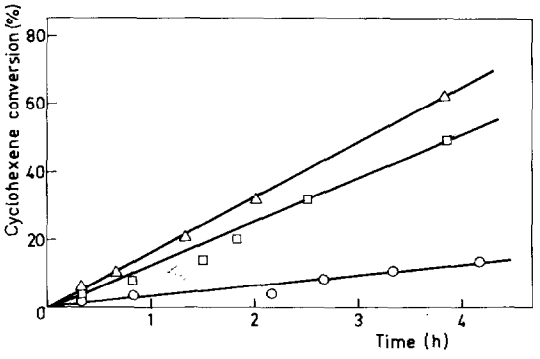

Fig. 6. Dependence of cyclohexene conversion at 573 K on reaction time for Ni–Mo/F(x)A catalyst: where x is 0.0 (○), 0.2 (□) and 0.8 (△).

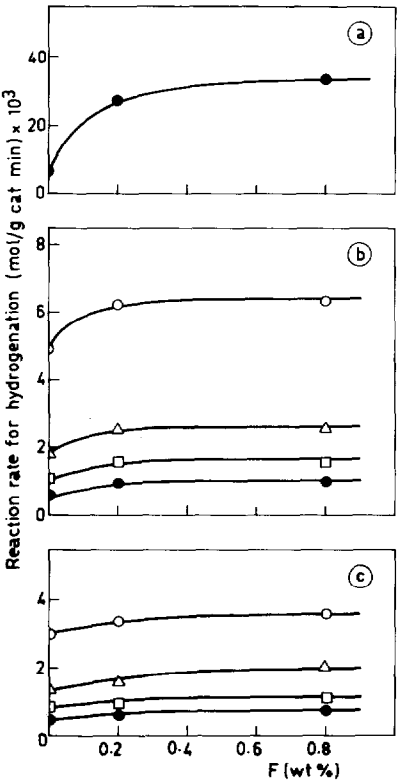

Fig. 7. Variation of the reaction rate for the hydrogenation of cyclohexene with fluorine content (a) Ni-Mo/F(x)A; (b) Co-Mo/F(x)A; (c) Mo/F(x)A. Reaction temperature: (●) 573 K; (□) 593 K; (△) 613 K; (○) 653 K.

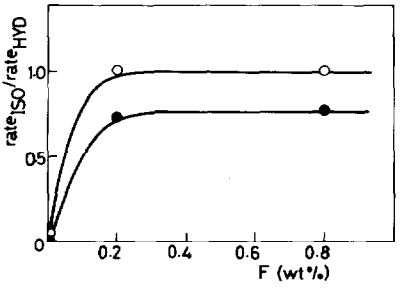

Fig. 8. Variation of the reaction selectivity as a function of fluorine content of the Mo/F(x)A catalyst at (○) 653 K and (●) 613 K.

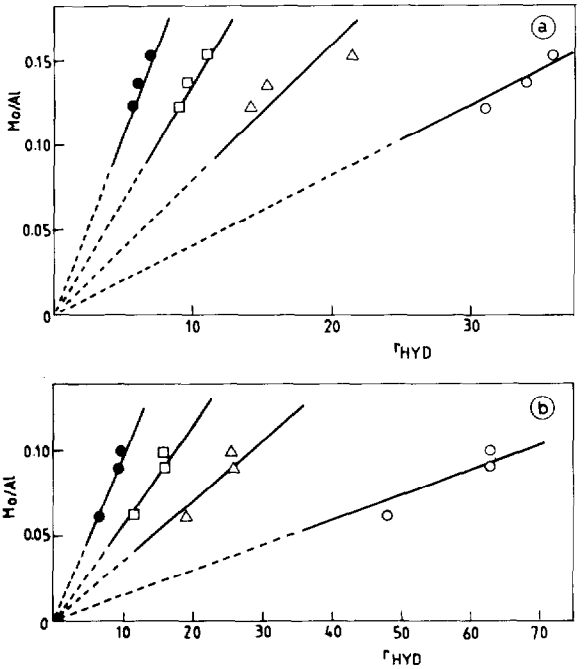

Fig. 9. Correlation between Mo-to-Al ratio and r_{HYD} for: (a) Mo/F(x)A; (b) Co-Mo/F(x)A at different reaction temperatures (Symbols as in Fig. 7).

fluorine incorporation on reaction selectivity is illustrated in Fig. 8. It is clear that the rate of isomerization increased enormously due to the fluorination. This becomes comparable to or slightly less than (depending on the reaction temperature) the rate of hydrogenation.

In order to check whether the catalytic activity of the Ni–Mo/F(x)A catalysts is a result of synergism, the Ni/F(0.2)A catalyst was also tested. The activity of this catalyst was found to be extremely low at reaction temperatures below 613 K. When it was appreciable, the predominant reaction was hydrogenation. Thus, at 573 K the r_{HYD} of the Ni/F(0.2)A catalyst was $2.9 \cdot 10^{-4}$, about a half of that of the Mo/F(0.2)A and ca. 100 times lower than that of the Ni–Mo/F(0.2)A catalysts, which indicates that a synergism effect occurs for the Ni–Mo/F(x)A catalysts.

DISCUSSION

Effect of fluorine on catalyst structure

On the basis of XRD and the BE values of F 1s, formation of AlF_3-like compounds on the present catalysts should be excluded, suggesting that fluorine is

well dispersed over the alumina surface. This finding is consistent with recent results of Okamoto and Imanaka [31] who showed that F^- ions were monomolecularly dispersed on fluorinated alumina up to a surface concentration of about $10 \cdot 10^{13}$ F^- cm^{-2}, which is close to the maximum F^- loading ($13.3 \cdot 10^{13}$ F^- cm^{-2}) used here. On the other hand, the BE of F 1s found for all the catalysts indicates that fluorine may not interact with Mo and promoters. However, from both XPS and IR results it is evident that the incorporation of fluorine influences the dispersion of both Mo and promoters. According to the BE of Mo $3d_{5/2}$ for the Mo/F(0.0)A catalyst (228.9 eV), upon sulfiding, oxidic Mo species were completely converted to small slabs of MoS_2, presumably of different sizes and number of layers. These are, presumably, distributed inhomogenously on the alumina surface, with some Mo-enrichment at the outer surface of alumina, as revealed by the higher XPS Mo-to-Al ratios than those predicted by a theoretical model for monolayer dispersion [28].

The prior incorporation of fluorine caused a slight increase in the Mo-to-Al ratio, which could reflect, in principle, major inhomogeneity, i.e. more molybdenum deposited on the outer alumina surface, and/or an actual improvement of Mo dispersion. The last interpretation is, however, more likely as the trend of the Mo $3d_{5/2}$/Mo $3d_{3/2}$ intensity ratio of Mo/F(x)A catalysts indicates that the fraction of non-reduced or non-sulfided Mo^{6+} species increases for Mo/F(0.2)A catalyst. For this catalyst, the relatively minor reducibility or sulfidation of MoO_3 precursors might be attributed to an increase in the interactions between molybdate and alumina caused by the increase in the dispersion. This explanation is consistent with the slight increase in the absorbance of NO found for the Mo/F(0.2)A catalyst (Fig. 3a). As the NO molecule probes Mo species placed both in inner pores and on the outer external surface, reflecting the size of the MoS_2 slabs [32], it can be concluded that fluorine provokes a slight increase in Mo dispersion for the Mo/F(0.2)A catalyst. For the Ni- and Co-promoted catalysts, since they were prepared by succesive impregnations (promoter last), it is expected that the previous fluorine effect of increasing Mo dispersion was not substantially changed. Indeed, Fig. 5b shows that the Mo-to-Al ratio increases with increasing fluorine content. Moreover, Fig. 3a shows that the absorbance of No and $Mo^{\delta+}$ species was, relatively, much larger for the Co–Mo/F(x)A ($x = 0.2$ or 0.8) catalysts than for the F-free counterpart, corroborating the conclusion based on XPS results. On the basis of NO and O_2 chemisorption data, similar results were previously found for Ni–Mo/F(x)A catalysts prepared by a procedure similar to that described here [3]. More recently [11,12] for catalysts where specifically fluorine was incorporated after deposition of Mo and Ni(or Co), it has been shown that fluorine causes generally an increase or a decrease in the dispersion of Mo and promoter, depending on the F^- content range used and the nature of the promoter.

A tentative explanation for the F-induced Mo dispersion, based on the de-

crease in the isoelectric point (IEP) after alumina fluorination and the different preference of adsorption of monomeric MoO_4^{2-} and polymeric $Mo_7O_{24}^{6-}$ oxyanions, has been suggested [3]. However, recent results on the adsorption of molybdates on modified alumina showed that the overall adsorption of the Mo oxyanions decreased by decreasing the IEP of the alumina upon fluorine incorporation [19]. Thus, factors other than chemical may contribute to the observed effect of fluorine on Mo dispersion. The partial solubilization of the alumina during the first NH_4F impregnation step may alter the dispersion of molybdate and promoters. A small fraction of the surface Al^{3+} cations is solubilized by fluoride treatment, which remains in solution until water removal by evaporation. After drying, those ions again precipitate as $Al(OH)_3$, thus forming a coating over the alumina surface. Upon calcination at 723 K, such a species becomes partially decomposed and provides new adsorption sites for molybdate partially decomposed and provides new adsorption sites for molybdate and promoters in the further impregnation sequence. This hypothesis is in agreement with the XPS results [Figs. 5a and 5b]. As the new alumina layer is generated, a quite different distribution of molybdena and promoter (Co or Ni) is expected to occur. Attention is paid to Co owing to its lesser abundance. On the basis of the solubilization–precipitation model for the coating of alumina, a larger proportion of promoter ions (Co^{2+}) would be lost for Co–Mo/F(x)A ($x=0.2, 0.8$) that for its Co–Mo/F(0.0)A counterpart as a greater number of alumina sites, able to form $CoAl_2O_4$ species through solid state reactions, are available in the former case. This interpretation is supported by the infrared spectroscopy of the NO adsorbed which indicated an important decrease (Fig. 3) of the octahedral Co^{2+}, where adsorption sites are usually assumed to take place, with subsequent increase of the exposure of molybdena. A similar behaviour would be expected for Ni–Mo/F(x)A catalyst. However, a slight increase of the Ni^{2+} exposure was still observed for Ni–Mo/F(0.2)A preparation. Due to the higher Ni content of the catalysts, rather than the Co content of its counterparts, this increase is reasonable and the loss of Ni in the $NiAl_2O_4$ spinel may be compensated for by a better dispersion of the remaining nickel oxide which then undergoes sulfidation. Such a distribution of Ni species cannot be unambiguously established by XPS because Ni 2p peaks become poorly resolved and broadened. However, as the BE of the Ni $2p_{3/2}$ at 853.7 eV of the Ni–Mo/F(0.2)A catalyst is close to that at 853.2 eV for Ni_3S_2, it results that the most abundant Ni species is well sulfided.

Effect of fluorination on catalytic activity

Activity results show clearly that fluorine incorporation in the catalysts leads to an increase in hydrogenation activity, which is appreciable for the unpromoted Mo, moderate for the Co-promoted, and considerably larger for the Ni-promoted catalysts. As the BE of Mo 3d levels for all catalysts were essentially

the same, the catalytic activity increase brought about by fluorination does not seem to be due to any electronic effect of F^- or a Mo–F interaction. This suggestion is also corroborated by the absence of a significant shift in the BE of the S 2p, F 1s and Ni $2p_{3/2}$ levels for all catalysts. In the case of the Co–Mo/F(x)A catalysts, the observed slight increase in the BE of Co $2p_{3/2}$ from 779.6 eV (for $x=0.0$) to 780.7 eV (for $x=0.2$) and then a subsequent decrease to 778.7 eV (for $x=0.8$) can be related more to changes in the dispersion of Co_9S_8 [12] than to an electronic effect.

From the fact that the catalytic activity and the dispersion of Mo and promoters are clearly changed by fluorine incorporation, it might be inferred, in principle, that the enhancement of hydrogenation activity is directly related to the dispersion increase. However, such a relationship cannot be drawn at first instance if the data are examined more closely. Thus, Fig. 9 shows that the Mo-to-Al XPS ratios and hydrogenation activities for the Mo/F(x)A and Co–Mo/F(x)A catalyst series correlate satisfactory, although following a different linear relationship for each catalyst series. However, the M-to-Al XPS ratios and hydrogenation activities correlate only roughly (not shown here), and do not go through the origin. This type of pseudo-linear correlation indicates that the dispersion of Mo and, especially, of promoter is not the key structural parameter which may control hydrogenation activity, but Mo dispersion is essential for it. At present, the idea more generally accepted is that the active sites for hydrogenation reactions reside at the edge planes of MoS_2, and their concentration depends primarily on the slab size. In this respect, it is important to consider the results of NO adsorption, as it has been stated that NO adsorption occurs exclusively at edge sites of MoS_2 [33]. It is significant that only a rough linear correlation between NO adsorption on Mo (Fig. 3) for the Co–Mo/F(x)A catalysts and their hydrogenation activity can be drawn, and no correlation between NO adsorption on exposed promoter atoms and hydrogenation activity is obtained. This lack of correlation, also found between NO adsorption and hexane hydrogenation activity on differently modified alumina-supported Mo catalysts [30,34], contrasts with reliable correlations between NO adsorption and HDS reactions reported. It appears once more that hydrogenation and HDS do not involve the same catalytic sites, as it has generally been reported in the literature (see, e.g., refs. 30 and 34 and references therein). Recent papers have provided evidence that the generation of different active sites is the result of some configurations of Mo ions and sulfur vacancies, three coordinatively unsaturated sites (CUS) being required for hydrogenation [35,36]. On this basis, and considering that in the present study the hydrogenation activity can be better correlated with the results of Mo dispersion than with those of promoter dispersion, one may speculate that the increase in hydrogenation activity induced by fluorine incorporation may predominantly be due to changes in Mo dispersion and the resulting variation in reducibility and sulfidation extent. Furthermore, since the Ni promoter ef-

fect is clearly manifest, besides an enhancement of Ni dispersion by fluorine incorporation, the primary improvement in Mo dispersion may subsequently lead to more Ni atoms located in edge positions of MoS_2 and, consequently, to facilitate the reduction of Mo by an electronic transfer from Ni to Mo. In the case of the Co–Mo/F(x)A catalysts, the effect is lessened because the Co content is relatively lower and the electronic transfer effect is also lower than for Ni.

Finally, the observed change in reaction selectivity for the Mo/F(x)A catalysts (Fig. 7) agrees with the parallel increase in acidity caused by fluorine incorporation (Fig. 1). In the case of the Ni–Mo/F(x)A catalysts, whose acidity is comparable to that of the Mo/F(x)A counterparts, the strong hydrogenation functionality of Ni controls reaction selectivity.

ACKNOWLEDGEMENTS

Financial support from CICYT, Project PB87-0261 and Programa de Cooperación Científica con Iberoamérica, M.E.C.; Spain, and CONACYT, Mexico, is gratefully acknowledged.

REFERENCES

1 P.M. Boorman, J.F. Kriz, J.R. Brown and M. Ternan in H.F. Barry and P.C.H. Mitchell (Eds.), Proc. Climax 4th Int. Conf. on Chemistry and Uses of Molybdenum, Climax Molybdenum Co., Ann Arbor, MI, USA, 1982, p. 192.
2 L.G. Tejuca, G.H. Rochester, A. López Agudo and J.L.G. Fierro, J. Chem. Soc., Faraday Trans. I, 79 (1983) 2543.
3 J.L.G. Fierro, A. López Agudo, L.G. Tejuca and G.H. Rochester, J. Chem. Soc., Faraday Trans. I, 81 (1985) 1203.
4 C. Muralidhar, F.E. Massoth and J. Shabtai, J. Catal., 85 (1984) 44.
5 P.M. Boorman, J.F. Kriz, J.R. Brown and M. Ternan, in Proc. 8th Int. Congr. Catal., Vol. II, Verlag Chemie, Weinheim, 1984, p. 281.
6 P.M. Boorman, R.A. Kydd, Z. Sarbak and A. Somogyvari, J. Catal., 96 (1985) 115.
7 P.M. Boorman, R.A. Kydd, Z. Sarbak and A. Somogyvari, J. Catal., 100 (1986) 287.
8 P.M. Boorman, R.A. Kydd, Z. Sarbak and A. Somogyvari, J. Catal., 106 (1987) 544.
9 K. Jiratova and M. Kraus, Appl. Catal., 27 (1986) 21.
10 C. Papadopoulou, C. Kordulis and A. Lycourghiotis, React. Kinet. Catal. Lett., 33 (1987) 259.
11 C. Papadopoulou and A. Lycourghiotis, P. Grange and B. Delmon, Appl. Catal., 38 (1988) 255.
12 H.K. Matralis, A. Lycourghiotis, P. Grange and B. Delmon, Appl. Catal., 38 (1988) 273.
13 T.R. Hughes, H.M. White and R.J. White, J. Catal., 13 (1969) 58.
14 P.O. Sockart, S.A. Selim, J.P. Damon and P.G. Rouxhet, J. Colloid Interface Sci., 70 (1979) 209.
15 T.C. Ho, Catal. Rev. Sci., 30 (1988) 117.
16 S.H. Yang and C.N. Satterfield, Ind. Eng. Chem. Process. Des. Dev., 23 (1984) 20.

17 G. Perot, S. Brunet and N. Hamze in M.J. Phillips and M. Ternan (Eds.), Proc. 9th Int Congress on Catalysis Calgary, Vol. 1, The Chemical Institute of Canada, Ottawa, 1988, Vol. 1, p. 19.
18 F.P.J.M. Kerkhoff, J.C. Ondejans, J.A. Moulijn and E.R.A. Matulewicz, J. Colloid Interface Sci., 77 (1980) 120.
19 F.M. Mulcahy, M. Houalla, and D.M. Hercules in M.J. Phillips and M. Ternan (Eds.), Proceedings 9th Int Congress on Catalysis Calgary, Vol. 4, The Chemical Institute of Canada, Ottawa, 1988, p. 1968.
20 F.E. Kiviat and L. Petrakis, J. Phys. Chem., 77 (1973) 1232.
21 R. Moné in B. Delmon, P.A. Jacobs and G. Poncelet (Eds.), Studies in Surface Science and Catalysis, Vol. 1, Preparation of Catalysts I, Elsevier, Amsterdam, 1976, p. 381.
22 G.L. Schrader and C.P. Cheng. J. Phys. Chem., 87 (1983) 3675.
23 K. Segawa and W.K. Hall, J. Catal., 76 (1982) 133.
24 A. López Agudo, F.J. Gil Llambías, J.M.D. Tascon and J.L.G. Fierro, Bull. Soc. Chim. Belg., 93 (1984) 719.
25 J. Vályon and W.K. Hall, J. Catal., 84 (1983) 216.
26 Y. Okamoto, H. Nakano and T. Shimokawa, J. Catal., 50 (1977) 447.
27 R.I. Declerck-Grimée, P. Canneson, R.M. Friedman and J.J. Fripiat, J. Phys. Chem., 82 (1978) 885.
28 F.P.J.M. Kerkhoff and J.A. Moulijn, J. Phys. Chem., 83 (1979) 1612.
29 R. López Cordero, N. Esquivel, J. Lázaro, J.L.G. Fierro and A. López Agudo, Appl. Catal., 48 (1989) 341.
30 J.L.G. Fierro, A. López Agudo, N. Esquivel and R. López Cordero, Appl. Catal., 48 (1989) 353.
31 Y. Okamoto, and T. Imanaka, J. Phys. Chem., 92 (1988) 7102.
32 J. Miciukiewicz, W. Zmierczak and F.E. Massoth, Bull. Soc. Chim. Belg., 96 (1987) 915.
33 K. Suzuki, M. Soma, T. Onishi and K. Tamaru, J. Electron Spectrosc. Relat. Phenom., 24 (1981) 283.
34 A.R. Saini, B.G. Johnson and F.E. Massoth, Appl. Catal., 40 (1988) 157.
35 S. Kasztelan, H. Toulhoat, J. Grimblot and J.B. Bonnelle, Bull. Soc. Chim. Belg., 93 (1984) 807.
36 S. Kasztelan, H. Toulhoat, J. Grimblot and J.B. Bonelle, Appl. Catal., 13 (1984) 127.